EFFECT OF THE CONTACT TANK GEOMETRY ON DISINFECTION EFFICIENCY

Bruno[1,*] P., Di Bella[1] G., De Marchis[1] M.

[1] University of Enna "Kore", Cittadella Universitaria 94100 Enna, Italy
*Corresponding Author

ABSTRACT - *Disinfection is a sanitary treatment present in both drinking water and wastewater treatment plants aimed at removing pathogenic microorganisms able to damage the human health. The focus of this study is to apply Computational Fluid Dynamics (CFD) to study and to improve the disinfection efficiency through the optimization of the hydrodynamics inside the disinfection tank. Numerous literature studies have shown that water flow inside traditional multichamber tanks is highly turbulent because of the development of large as well as small vortices in which flow velocity decreases or even vanishes (dead zones). These turbulent phenomena are responsible of an increase of the real residence time, compared to the theoretical one, causing poor disinfection and the development of unwanted by-products. In the present analysis, Large Eddy Simulation (LES) is used to simulate three-dimensional turbulent flow and disinfectant transport in different contact tanks using a structured finite-volume discretization. The results show how the baffles' geometry, as well as the design of technical and construction details, influences the hydraulic retention time of the disinfectant, varying the disinfection efficiency. In particular, the creation of horizontal baffles inside the vertical baffle chambers reduces the free space and extends the flow path. This reduces both short circuits and recirculation zones bringing the flow closer to the ideal plug-flow condition.*

Keywords: *disinfection, Computational Fluid Dynamics (CFD), Large Eddy Simulation (LES), contact tank, baffle design.*

1. Introduction

The most common disinfection methods in water treatments involve the use of chemicals and, in particular, chlorine and its compounds and ozone. Disinfection treatments through chemical reagents are generally carried out inside rectangular contact tanks where the presence of parallel baffles forces the flow to follow a serpentine path with 180° flow inversions that increase the contact time of the bacteria with the chemical reagent used for disinfection [1]. Fluid motion in serpentine disinfection tanks, like most of fluid-dynamic processes in real systems, is a turbulent process (i.e. a nonstationary, irregular and chaotic motion) characterized by the presence of eddies of different sizes and speeds, which continuously change.

Plug-flow reactor is undoubtedly the most widely used type of reactor in chemical disinfection treatments. In these systems, the tracer concentration within each cross-section is constant, while the dispersion in the longitudinal direction is almost zero. In this way, the real hydraulic residence time (HRT) of the plug-flow reactor is equal to the theoretical one established in the design phase. Plug-flow reactors ensure, therefore, a perfect hydraulic and sanitary performance of water disinfection processes [2].

Traditional disinfection processes take place inside reactors with rectangular chambers separated by horizontal or vertical baffles. This geometric configuration causes the development of several areas characterized by whirling motions [3] where the speed decreases or even vanish causing the disinfectant entrapment [4]. These turbulent phenomena deeply modify the operating system with respect to the ideal plug-flow condition and, since the recirculation zones occupy a considerable portion of the tank volume, they modify the real hydraulic residence time from the theoretical one [5]. Even though the baffles are able to avoid the short-circuiting phenomena which occurs when particles pass through a reactor quicker than the theoretical HRT, the wide vortices within the cavities trap disinfectants and pathogens, which are then retained in the tank for a longer period than the theoretical hydraulic residence time [5]. The occurrence of such flow patterns has a detrimental effect on the overall treatment efficiency since an increase in contact time could cause the generation of harmful by-products, while its decrease could cause a poor disinfection [6]. This happens in particular in the case of chlorine disinfection where the formation of disinfection by-products (DPBs) depends on the disinfectant's concentration in the tank and on its reactions with other water constituents [7].

In the case of disinfectants that do not produce disinfection by-products, on the other hand, previous studies show that increasing the contact time is favorable [8].

Recently, Computational Fluid Dynamics (CFD) is increasingly applied to analyze elements of Water Treatment Plants, due to the ability of a numerical approach to achieve fast and economic results with respect to the conventional experimental methods [4,5,9]. The most analyzed element is perhaps the disinfection unit. Different chamber shapes have been simulated [3,10–12] and different turbulence models have been employed, showing how both the shape of the domain as well as the turbulence model greatly influence the results [10,13,14]. In many studies Reynolds Averaged Navier-Stokes (RANS) based turbulence models have been used with significant time savings, as they require lower computational costs [15]. However, even though RANS simulations are able to predict the mean flow inside the tank, it has been demonstrated [13] that they are not able to predict smaller scale eddies that cause disinfectant entrapment at corners. These recirculation zones could be better simulated with Large Eddy Simulation (LES) models capable of accurately assessing the variation of turbulent fluctuations [16,17]. Undoubtedly, LES techniques require the use of a finer resolution mesh and therefore they involve higher computational costs. Nevertheless, nowadays, thanks to recent technological advances, the scientific community is paying more and more attention to LES techniques, which allow greater precision and reliability of results, also in industrial applications where usually RANS has been used [18]. In terms of computational costs, LES represents a valid compromise between RANS and Direct Numerical Simulation (DNS) techniques. DNS is, in fact, a numerical method where all the turbulence scales of motion are directly resolved, without the introduction of specific turbulence models. Unfortunately, DNS requires a huge amount of compute cells resulting in high computational costs. On the other hand, LES is designed to resolve the large scales, responsible for the production of kinetic energy, whereas the small scales, responsible for the energy dissipation, are modelled with the consequent reduction of computational costs. Furthermore, LES models are the only ones able to accurately simulate the disinfectant mixing with the flow [4,9], which is of fundamental importance in tracer studies. In light of all this, in the present analysis, LESs are applied to investigate disinfection efficiency in multichamber reactors, with the aim of optimizing the tank design to improve disinfection hydraulic and chemical performances of new or existing reactors.

As previously mentioned, in the literature there are numerous examples of computational fluid dynamics studies conducted with the aim of optimizing the hydrodynamics in disinfection tanks. All these studies focused the attention on the effect of the contact tank geometries, thus to reach an ideal plug-flow condition. The main objective of this study is to provide further insights of this issue exploring alternative geometries able to optimize the hydraulic performance. A fundamental challenge is to find a simple geometry for new tanks or for the upgrading of existing tanks. The hydrodynamic improvement of the tank is evaluated considering the hydraulic efficiency indicators typical of these studies. The results showed that the number and arrangement of the baffles, the width of the chambers and the number of inversions are responsible of the disinfection efficiency.

The paper is organized as follows. In Section 2, the physical problem and the numerical model solver is described. Section 3 presents the validation test cases, where geometries already studied in literature were reproduced and compared. In Section 4, the results obtained in the new designed contact tanks are shown and discussed. In the final section main findings are summarized and conclusions are drawn.

2. Numerical Approach

In the study of treatment plants, the application of numerical techniques allows to reduce the design times and to choose the optimal hydrodynamic configuration. Nowadays this is a fundamental point for the scientific community that works in these areas since it would help engineers in improving facility designs and consequently bring economic benefits before construction.

2.1 Governing Equations of Fluid Flow

Turbulent flows, as previously mentioned, are resolved using LES approach, based on the numerical solution of the filtered continuity and momentum equations, given by:

$$\frac{\partial u_i}{\partial x_i} = 0 \tag{1}$$

$$\frac{\partial u_i}{\partial t} + u_j \frac{\partial u_i}{\partial x_j} = -\frac{1}{\rho}\frac{\partial p}{\partial x_i} + \nu \frac{\partial^2 u_i}{\partial x_j \partial x_j} + f_i \tag{2}$$

where u_i and x_i are velocity and position in the i-th direction, t is time, ρ is fluid density, p is pressure, ν is the kinematic viscosity, and f_i represents the force per unit of mass in the i-th direction.
The governing equations are resolved using the second-order accurate numerical model OpenFOAM (Open source Field Operations and Manipulations - CFD Direct Ltd., Reading, UK). Specifically, the transient solver pimpleFoam, available for incompressible and turbulent flow of Newtonian fluids, has been used in this study. This solver is a combination of PISO (pressure-implicit split operator) and SIMPLE (semi-implicit method for pressure-linked equations) solvers. The PIMPLE algorithm is composed of an implicit momentum predictor and several pressure-velocity correctors. In the PIMPLE loop, the velocity equations are firstly solved by using the velocity and pressure fields of the previous time step, known as momentum predictor. The velocity and pressure are corrected several times afterwards to satisfy mass conservation. Specifically, the algorithm solves a pressure equation, to enforce mass conservation, with an explicit velocity correction to satisfy the momentum conservation. Different LES subgrid models are available for incompressible flows. In this case, Wall-Adapting Local Eddy-Viscosity (WALE) model has been used, where the eddy viscosity is modeled by:

$$\mu_t = \rho L_S^2 \frac{\left(S_{ij}^d S_{ij}^d\right)^{3/2}}{\left(\bar{S}_{ij}\bar{S}_{ij}\right)^{5/2} + \left(S_{ij}^d S_{ij}^d\right)^{5/4}} \tag{3}$$

where μ_t is the subgrid-scale turbulent viscosity, L_s is the mixing length for subgrid scales, $\bar{S}_{ij}$ is the rate-of-strain tensor for the resolved scale defined by:

$$\bar{S}_{ij} = \frac{1}{2}\left(\frac{\partial \bar{u}_i}{\partial x_j} + \frac{\partial \bar{u}_j}{\partial x_i}\right) \tag{4}$$

In the WALE model L_s and S_{ij}^d are respectively defined as:

$$L_s = min\left(kd, C_w V^{1/3}\right) \tag{5}$$

where k is the von Kármán constant, d is the distance to the closest wall, C_w is the WALE constant equal to 0.325 and V is the volume of the computational cell.

$$S_{ij}^d = \frac{1}{2}\left(\bar{g}_{ij}^2 \bar{g}_{ij}^2\right) - \frac{1}{3}\delta_{ij}\bar{g}_{kk}^2 \tag{6}$$

with $\bar{g}_{ij} = \frac{\partial \bar{u}_i}{\partial x_j}$

2.2 Governing Equations for Tracer Transport

The hydraulic efficiency of multichamber reactors in terms of disinfection capacity is evaluated considering the flow of a non-reactive tracer inserted inside the tank to obtain the mean residence time. In CFD simulations, a passive scalar tracer is a conservative substance that is transported along the volume of fluid without interfering with local hydrodynamics [19]. Tracer studies are performed by inserting the tracer at the reactor inlet and measuring the response at the outlet in order to obtain residence time statistics [20]. In this specific case, the tracer is injected with a uniform distribution from the inlet for a time of 2.5 seconds and the outlet concentration variation is monitored throughout the numerical simulation. In order to simulate the transport of the conservative tracer, standard solver pimpleFoam is modified including the following advection-diffusion equation:

$$\frac{\partial \bar{C}}{\partial t} + \overline{u_j}\frac{\partial \bar{C}}{\partial x_j} = \frac{\partial}{\partial x_j}\left((D + D_t)\frac{\partial \bar{C}}{\partial x_j}\right) \tag{7}$$

where $\overline{u_j}$ is the velocity component along the j-direction (x, y and z), t is the time, x_i and x_j represent the Cartesian coordinates, $\bar{C}$ is the filtered tracer concentration, D is molecular diffusivity, which is negligible compared to turbulent diffusivity D_t. The turbulent diffusivity can be computed as $D_t = \mu_t / S_c$ where μ_t is eddy viscosity calculated in (3) while S_c is the turbulent Schmidt number which is set to 1000 in order to maintain the same ratio between the water molecular viscosity and the tracer mass diffusivity used in the experiments by Kim et al. [6,21].

2.3 Flow Domain, Simulation Setup and Boundary Conditions

The reactor model used in the present study to simulate flow and tracer transport in disinfection treatments, has geometric characteristics identical to those used in the other literature studies, in order to make possible a comparison of the results obtained for the validation of the numerical model. The most recent studies concerning multichamber reactors are based on physical tracer experiments conducted by Kim et al. [6]. The laboratory scale contactor used in the aforementioned study consisted of 12 chambers, while the same author performed computational simulations on a truncated version of the reactor [4] also used in the present study in order to reduce the computational cost. In the truncated reactor, the number of chambers is reduced from 12 to 4 while maintaining the same chamber width equal to 0.113m. In this way, the reactor has an overall longitudinal length of 0.48 m and a width of 0.23 m. The deflectors have a height of 0.18m while the water reaches a height of 0.21m inside the reactor as shown in Figure 1.

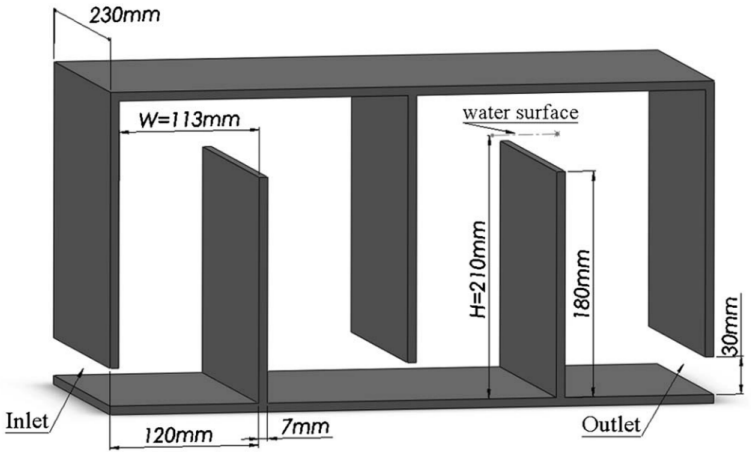


Figure 1 *Three-dimensional schematic view of the computational domain* [13].

The water enters the reactor with a constant discharge of *0.2 l/s* from the inlet located at the left of the first chamber and flows from the outlet on the opposite side of the multichamber. The computational domain is decomposed through a Cartesian grid (Figure 2) using 210 x 90 x 90 cells in the streamwise, spanwise and wall-normal directions respectively, in analogy with the study of Demirel and Aral [2], for a total of 1,701,000 cells. The cells size was determined following a sensitivity analysis, establishing a greater refinement of the grid near the bottom and baffle walls in order to resolve steep velocity gradients.

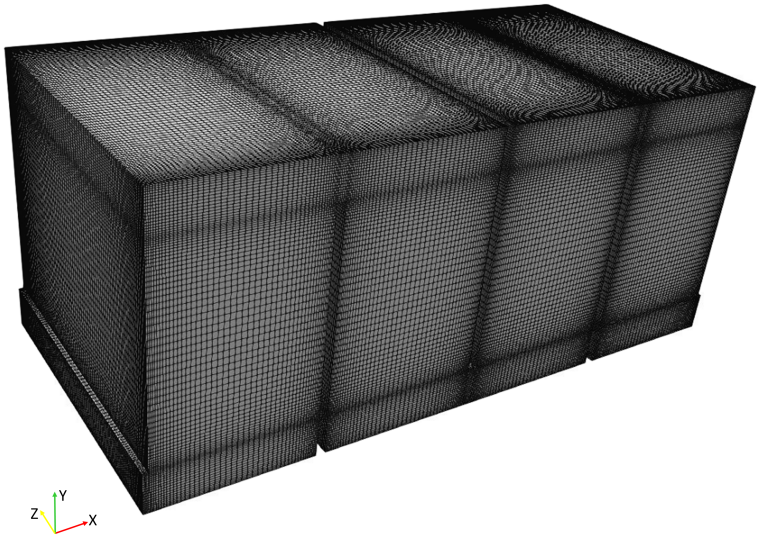


Figure 2 *Three-dimensional view of the structural mesh.*

In order to compare the numerical results with the previous literature studies, the same boundary conditions have been applied to the domain. In particular, the effects of roughness on the walls have been neglected and zeroGradient and no-slip conditions have been imposed on the walls for pressure and velocity respectively. Other boundary conditions available in OpenFOAM and applied on the bottom and on the walls are kqRWallFunction and nutkWallFunction for the turbulence kinetic energy and for the turbulence viscosity respectively. As previously mentioned, in the present study numerical simulations have been performed on the truncated version of the physical domain studied by Kim et al. [6] to reduce the computational time. In order to ensure the validity of the numerical simulation, periodic boundary conditions in the streamwise direction have been applied for velocity. This boundary conditions make the results independent on the inlet turbulence intensity avoiding unwanted flow disturbances that occur when different boundary conditions are applied to the inlet and outlet [10]. A uniform tracer concentration is injected into the tank applying a fixedValue boundary condition for the tracer, in such a way that the scalar enters uniformly from the entire inlet cross section, while zeroGradient boundary condition is used at the outlet and walls. Symmetry boundary condition is finally imposed on the upper face of the domain since free-surface effects are negligible [4,22].

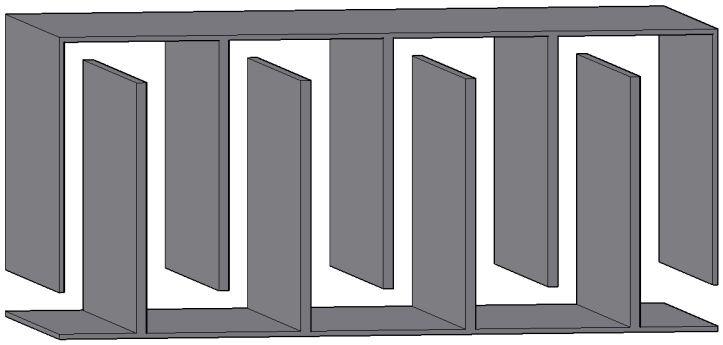
Numerical simulations are conducted using OpenFOAM code, which solves the governing equations through the finite volume method. For the temporal discretization of the governing equations, the second-order *backward* scheme is used. A 0.005 s time step is set to maintain the Courant-Friedrich-Levy (CFL) number below 0.5. As regards the space, *linearUpwind* and *Gauss linear* schemes are used for the treatment of the convective and diffusive terms respectively, so that the overall accuracy of the numerical method is second order.

Initially, the flow inside the reactor was simulated without the tracer for a time of 300 s in order to allow the flow field stabilization excluding the wake fluctuations generally observed during the initial phases of a simulation [2]. Once the flow field is established, the tracer is released inside the tank for a period of 2.5 s and the simulation is run for an additional 330 s to ensure that almost all the injected tracer passes through the outlet.

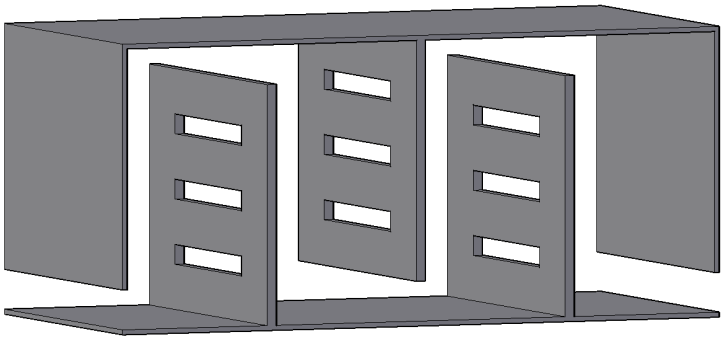
3. Validation of the numerical procedure

The aim of this study is to analyze hydrodynamics inside disinfection tanks characterized by technical and construction details allowing the flow to be brought closer to the ideal plug-flow condition and therefore optimizing the efficiency of the disinfection process. In light of this, literature studies have shown that it is possible to avoid the development of short circuits and recirculation phenomena by increasing the number of compartments [11], while making slots in the baffles it is possible to increase mixing in the chambers reducing dead zones [23]. Before proceeding to the analysis of the flow inside tanks having different characteristics from the traditional ones, it was necessary to validate the accuracy of the LES approach and the numerical methods used through a comparison with previous literature studies.

In order to validate the numerical procedure, three different reactors, already analysed in literature, have been tested: the traditional four-chamber reactor shown in Figure 1, identified below as NW (normal chamber width); the eight-chamber reactor (Figure 3a) obtained by doubling the number of baffles, thus halving the width of the chambers and therefore called HW (half chamber width); the reactor model presented by Aral and Demirel (2017) in the study "Novel Slot-Baffle Design to Improve Mixing Efficiency and Reduce Cost of Disinfection in Drinking Water Treatment" characterized by the presence of three slots for each baffle and hereafter identified as slot-baffle (Figure 3b).



(a)

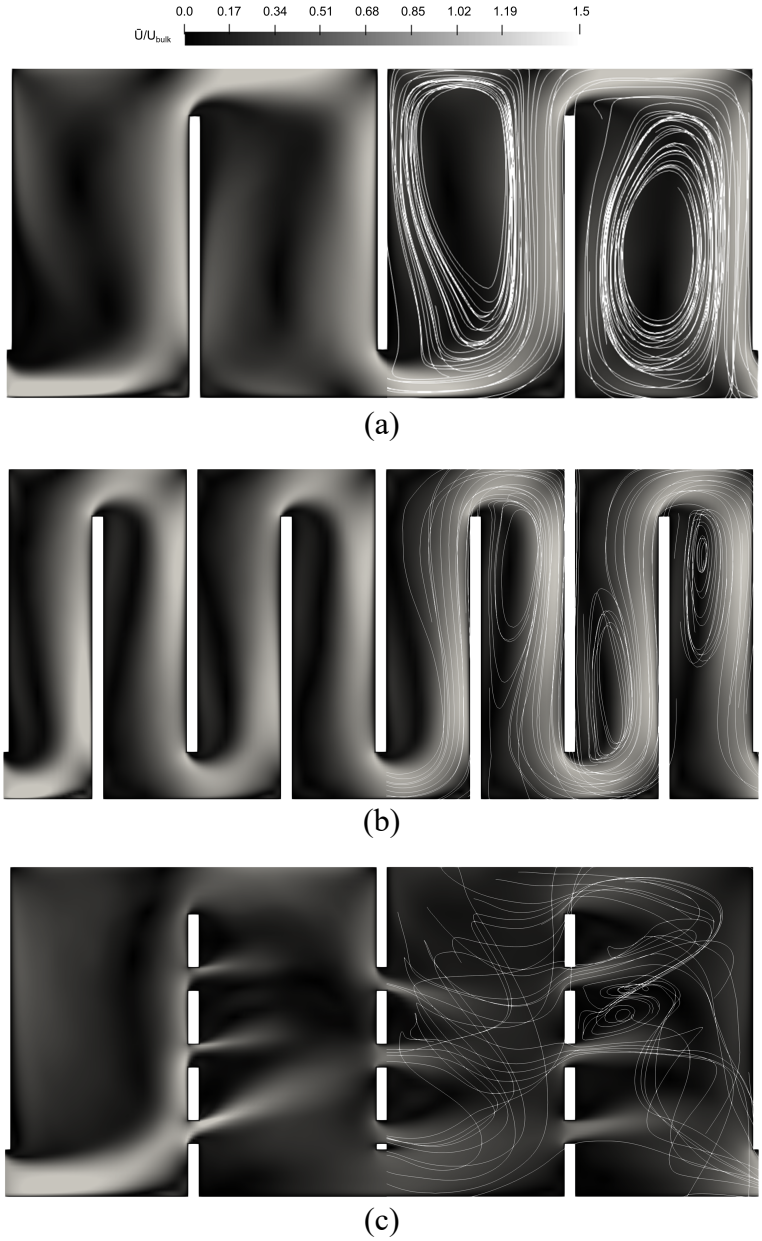


(b)

Figure 3 *Layout of (a) half chamber width (HW) and (b) slot-baffle reactors.*

220 *3.1 Flow Characteristics*

221 Figure 4 presents the time-averaged absolute velocity distribution along with two-dimensional
222 streamlines depicted in the last two chambers of each figure.



229 **Figure 4** *Time-averaged absolute velocity and streamlines (in the right half of the tank) in the center-plane (z /L=0.5)*
230 *of the chambers for (a) NW model; (b) HW model; and (c) slot-baffle model.*

231 Figure 4a shows how the NW reactor is characterized by a preferential serpentine flow at greater
232 speed (white contours), which extends near the right side of each chamber and suggests the occurrence
233 of short circuits inside the reactor. When the flow leaves a chamber, its velocity increases with respect
234 to the theoretical average (U_{bulk}) due to the presence of the crest of the baffles. This area is therefore
235 characterized by the presence of a sort of "jet" at high speed that extends from one room to another.
236 The high flow velocity determines the passage of a portion of water through the entire length of the
237 contactor in much shorter times than the average hydraulic residence time, with consequent short
238 circuit and therefore a reduction in disinfection efficiency. The streamlines show that the entire central
239 part of the chambers is occupied by a large recirculation zone. A small secondary recirculation area
240 is observed, instead, at the corners between the bottom and the baffle walls, while near the water
241 surface no recirculation occurs. Finally, a small recirculation cell appears near the baffles free end.

The ability of the LES to capture the presence of this last recirculation zone explains why the latter is preferred to RANS simulation which is unable to simulate smaller scale eddies at the entrance of the chambers [13].

Figure 4b shows that the HW reactor has flow characteristics similar to the NW reactor. However, by halving the chamber width, the size of the primary recirculation zone is considerably smaller, occupying approximately half of the chamber. There is again a small secondary recirculation zone at the corners between the bottom and the walls of the deflector and, unlike the NW model, another small recirculation cell appears at the corners near the free surface.

Finally, Figure 4c shows that the presence of slots in the baffles improves the overall mixing efficiency of the contact tank since when the flow exits from the slot hit the recirculation zone and increases the mixing downstream the deflector, avoiding short-circuits and the excessive permanence of the disinfectant trapped in the recirculation and dead zones.

The qualitative comparison of the contour and of the streamlines achieved in the present simulations are in good agreement with the results observed in the literature of reference. In order to confirm the validity of the method, further quantitative comparison based on velocity and concentration profiles are presented below.

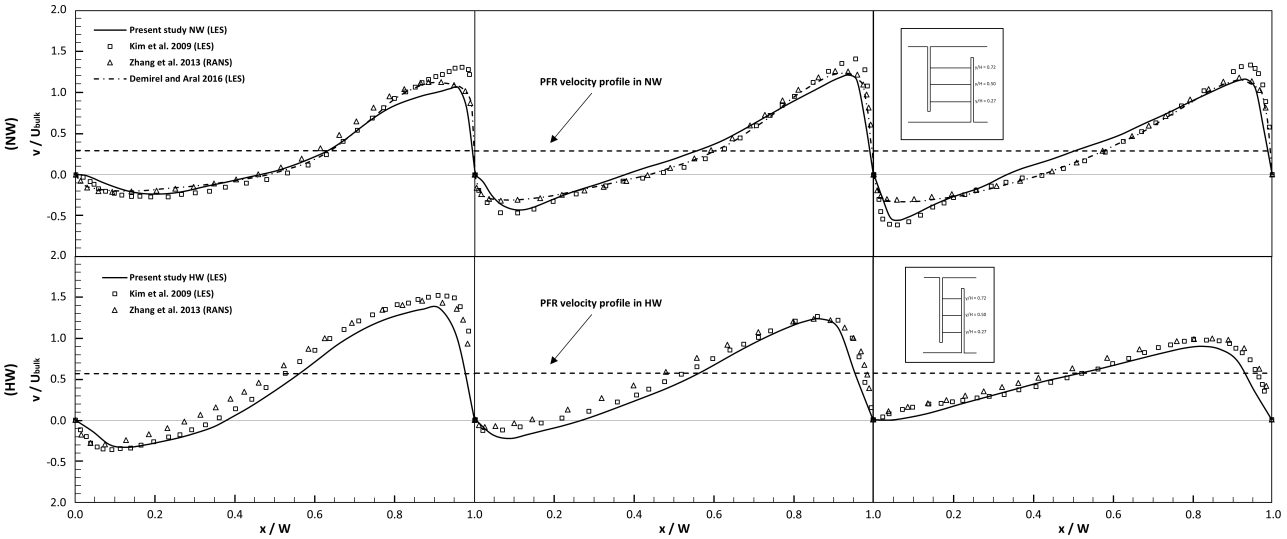


Figure 5 *Vertical velocity component across the chamber width of the different models and at different depths: (a) y/H = 0.27; (b) y/H = 0.5; (c) y/H = 0.72.*

For the validation of the numerical method, the velocity profiles obtained across the chamber width have been compared with literature data. For each reactor Figure 5 shows the normalized vertical velocity profiles obtained in a chamber at three different vertical heights. The results obtained are in good agreement with the data present in the literature for each model of reactor. Specifically, at all three depths investigated in NW model, the y-velocity varies through the chamber passing from negative to positive values. This happens because the presence of recirculation and dead zones prevents a uniform distribution of speed. As it is possible to observe, for NW and HW models the y-velocity in each chamber is greater along the right wall in correspondence with the preferential path followed by the flow. However in HW model, the y-velocity vector exhibits the greatest change of direction at depth $y/H = 0.27$, since the recirculation zone occupies only a small part in the bottom of the chamber. On the contrary, at the depth $y/H = 0.5$ the negative values of the y-velocity decrease, disappearing completely at $y/H = 0.72$. Finally, as regards the slot-baffle model, the jet that comes out of the slots creates a mixing that disturbs the dead and recirculation zones. For this motive, the direction change of the y-velocity vector is small at all the depths investigated and the velocity profiles (not shown here) assume a pseudo-horizontal trend that approaches that of an ideal plug-flow reactor (PFR).

3.2 Tracer analysis

The hydraulic efficiency of disinfection tanks is generally evaluated considering the flow of a passive scalar tracer injected from the inlet for a time of 2.5 seconds. The tracer distribution analysis is based on the examination of the RTD (Residence Time Distribution) and CRTD (Cumulative Residence Time Distribution) curves obtained at the outlet. Figure 6 shows that also in this case the results obtained are in perfect agreement with the literature data for the three models studied. In particular, the first peak of the normalized RTD graph obtained for the NW model indicates that high quantities of tracer leave the reactor after a shorter time than the theoretical hydraulic residence time τ. This confirms that conventional reactors suffer from short-circuit phenomena that reduce disinfection efficiency. The second peak, on the other hand, appears due to the presence of the recirculation areas that trap the tracer delaying its release. In the HW model, the second peak of RTD completely disappears due to the minimization of the recirculation zones, whereas the first peak moves to the right since the reduction of the chamber width reduces the short-circuiting effects. The RTD trend is getting closer to the plug-flow ideal one in the case of the slot-baffle model where the peak value is significantly smaller and appears even later and closer to the theoretical hydraulic residence time.

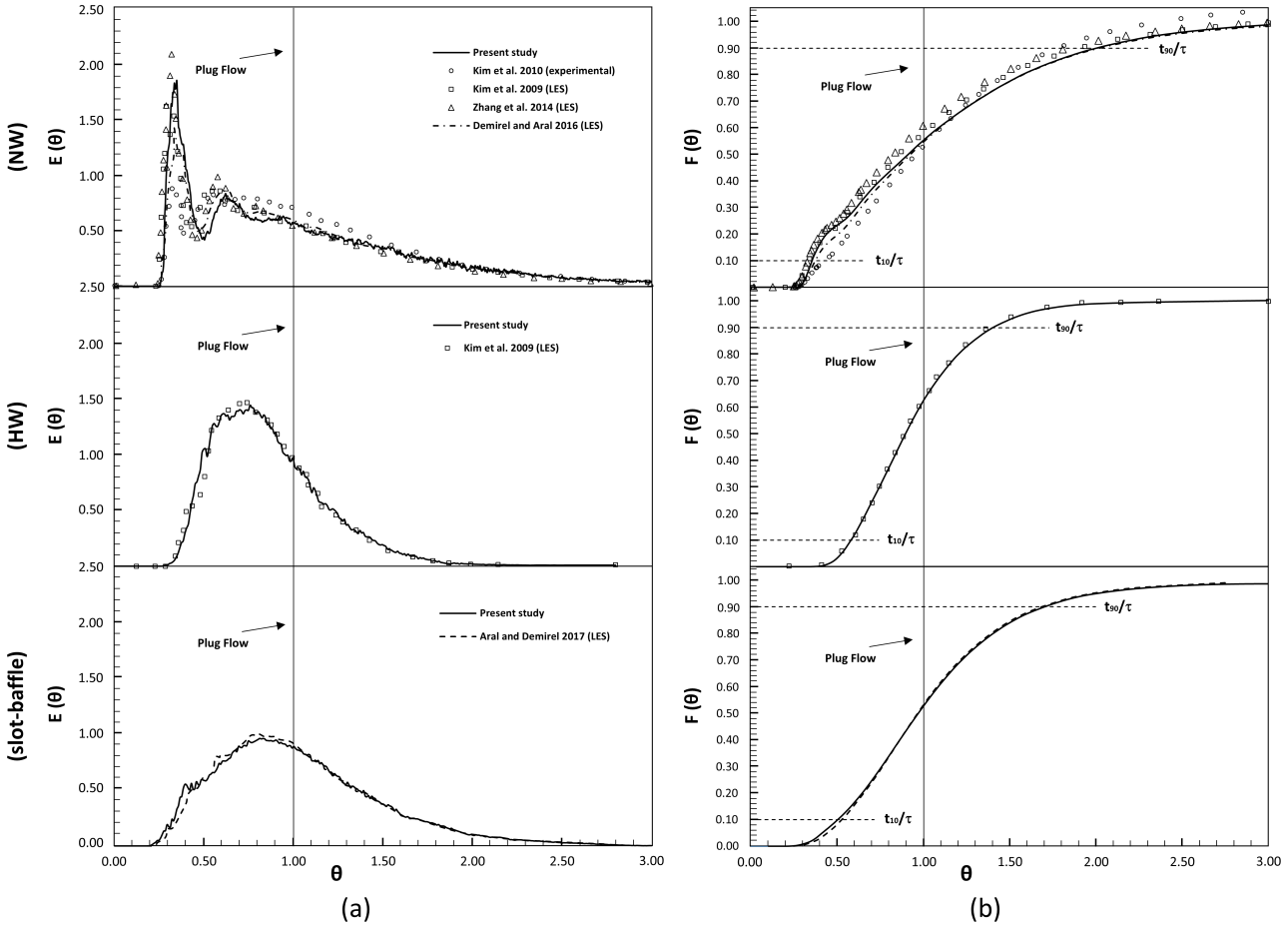


Figure 6 *Tracer analysis results obtained for the three reactor models: (a) normalized RTD plot and (b) cumulative normalized RTD plot.*

In the abscissa of RTD plot there is $\theta = t/\tau$ which is the nondimensionalized time with respect to the theoretical mean residence time ($\tau = V/Q$), while in the ordinate there is the tracer concentration which is nondimensionalized using:

$$E(\theta) = \frac{C}{\frac{C_{init} \cdot T_{release}}{\tau}} \tag{8}$$

where $C_{init} = 1$ is the uniform concentration of tracer injected at the inlet and $T_{release}$ = 2.5 s is the injection period. Cumulative normalized RTD plot is obtained by integrating the RTD curve:

$$F(\theta) = \int_0^\infty E(\theta) d\theta \tag{9}$$

From the cumulative RTD plot, it is possible to determine the indices usually used to evaluate the hydraulic and mixing efficiencies of contact tanks. Table 1 shows the comparison between literature data and the values of the Hydraulic Efficiency Indicators (HEI) considered in the present study. In particular, t_{10}/τ and t_{90}/τ represent the normalized times, starting from the introduction of the tracer, respectively necessary for the passage through the outlet of 10% and 90% of the mass of the tracer injected; the Morrill coefficient is defined as $Mo = t_{90}/t_{10}$, and is an indicator of the mixing degree in the tank [24]; σ^2 is the dispersion index and represents the variance of the RTD curve. The dispersion index is defined as:

$$\sigma^2 = \frac{\sigma_t^2}{t_g^2} \tag{10}$$

with

$$\sigma_t^2 = \tau^2 \cdot \frac{\int_0^\infty \theta^2 E(\theta) d\theta}{\int_0^\infty E(\theta) d\theta} \tag{11}$$

and

$$t_g = \tau \cdot \frac{\int_0^\infty \theta E(\theta) d\theta}{\int_0^\infty E(\theta) d\theta} \tag{12}$$

where σ_t^2 is the variance of the RTD curve and t_g is the normalized time to reach the centroid of the effluent curve [25]. As it is possible to observe from the table, the HEI values of the three reactor models here analyzed are in agreement with the CRTD curves obtained in literature physical experiments and computational simulations.

Table 1 *Hydraulic Efficiency Indicators for the three reactor models.*

	NW			**HW**			**slot-baffle**		
Study	t_{10}/τ	Mo	σ^2	t_{10}/τ	Mo	σ^2	t_{10}/τ	Mo	σ^2
Kim et al. 2010 (experimental)	0.420	4.222	1.308	-	-	-	-	-	-
Kim et al. 2009 (LES)	0.332	5.821	1.356	0.518	2.446	1.137	-	-	-
Zhang et al. 2014 (RANS)	0.321	5.629	1.383	-	-	-	-	-	-
Demirel and Aral 2016 (LES)	0.366	5.512	1.336	-	-	-	-	-	-
Aral and Demirel 2017 (LES)	-	-	-	-	-	-	0.528	3.191	1.183
Present LES	0.347	5.758	1.361	0.394	3.285	1.141	0.503	3.383	1.194

4. Performance of the new designed reactor with horizontal baffles

The results shown in the validation section, showed how the chamber width (HW reactor model) is responsible of the disinfection process improvement, reducing the short circuit effects and the

development of recirculation zones and bringing the flow closer to the ideal plug-flow condition. For this reason in the present study, focused to design new geometrical chambers able to optimize the hydraulic and sanitary efficiencies, new contact tanks were analysed thus to reduce the dimension of the contact tank chambers. Figure 7 depicts the proposed geometries where horizontal baffles are added to the classical vertical ones. These extremely regular geometries are simple to construct or possibly to implement in existing tanks with the aim of extending the flow path, bringing the hydraulic residence time closer to the theoretical ideal one.

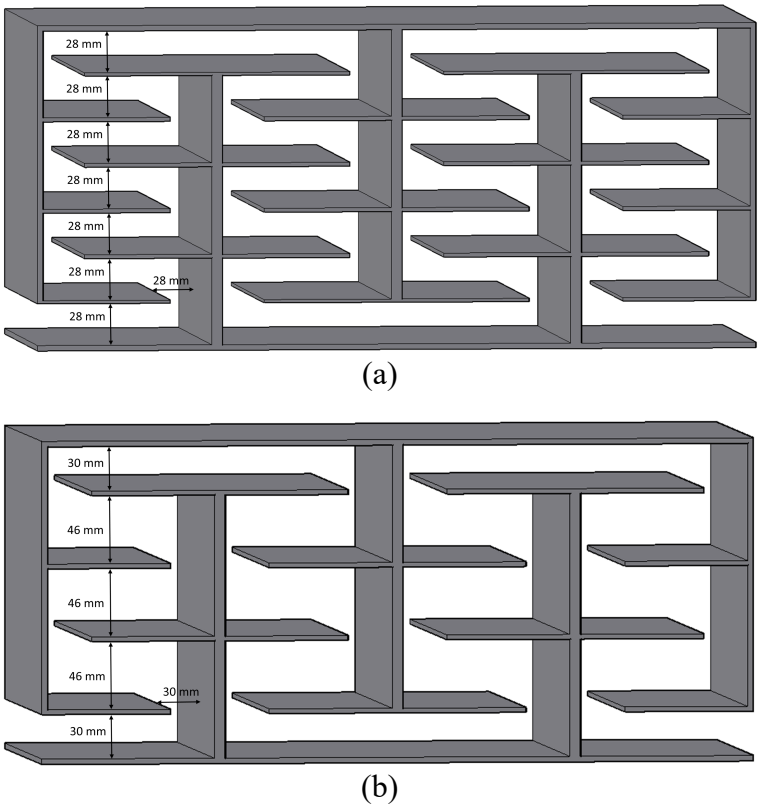


Figure 7 *Three-dimensional view of (a) constant section and (b) variable section horizontal baffled reactors.*

In Figure 7a, the reactor model is designed thus to ensure the same dimension of the flow path, equal to 28 cm. The same height is also chosen for the inlet section. On the other hand, in the second tested geometry, shown in Figure 7b, a variable section through which the flow passes is considered.
Figure 8 shows the streamlines superimposed to the contour of the non-dimensional velocity. The streamlines, compared with those observed in Figure 4, show how the presence of the horizontal baffles reduces the development of dead zones and the recirculation regions; moreover, the disinfectant is forced to remain inside the reactor for a longer time, bringing the flow closer to the ideal plug-flow condition. It can be thus observed that the introduction of horizontal baffles improves the disinfectant dispersion.
Comparing the two new designs plotted in Figure 8, it is evident how the number of horizontal baffles determines variations in the recirculation regions, affecting the turbulent mixing and the disinfectant dispersion.

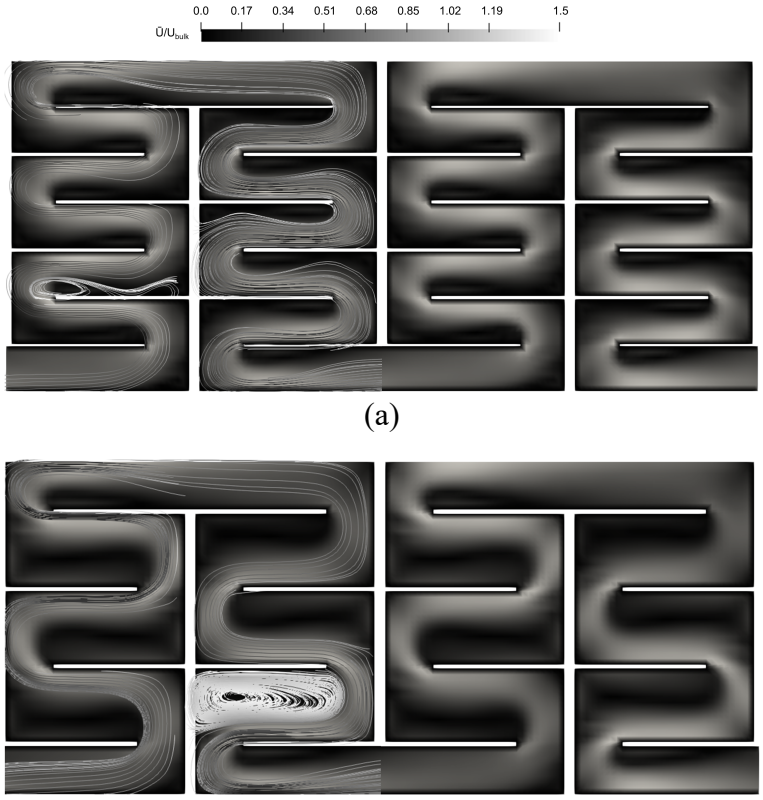


Figure 8 *Time-averaged absolute velocity and streamlines (in the left half of the tank) in the center-plane (z /L=0.5) of (a) constant section model and (b) variable section model.*

In order to investigate on the performance of the new designed contact tanks, the RTD curves and the cumulative normalized RTD curves are plotted in Figure 9a and 9b, respectively. The figure shows how the horizontal baffles are responsible of the disappearance of the second peak, evident in the conventional contact tank at $\theta = 0.65$. This is due to the dead zones reduction, where usually the disinfectant remains trapped and released after times. Moreover, the single peak of the curve shifts to the right and approaches to $\theta = 1$, indicating a considerable reduction in short-circuit effect.
Focusing on the two new designs with horizontal baffles, it can be observed how constant section reactor allows a greater shift of the peak towards the ideal condition with an almost impulsive behavior. This result is in agreement with the streamlines shown in Figure 8, where it was observed a reduction of recirculation regions compared with those occurring in the variable section reactor.

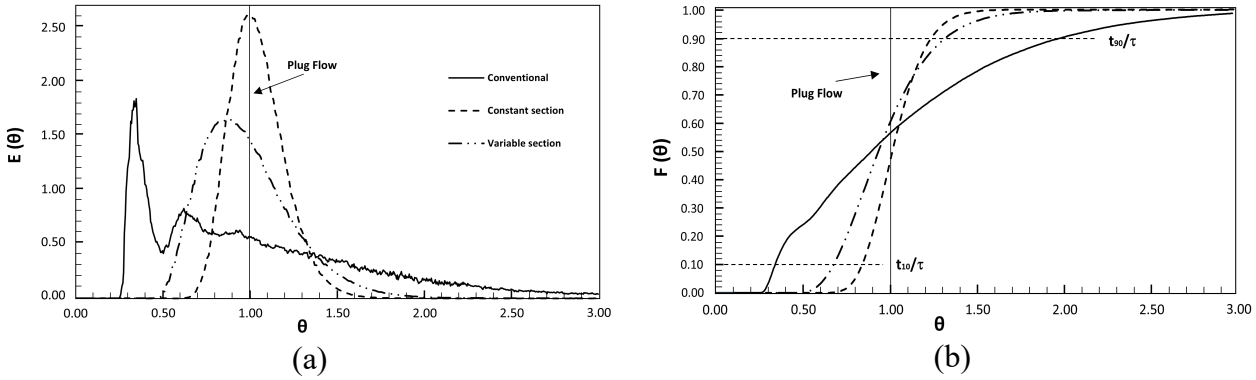


Figure 9 *Tracer analysis results obtained for the two horizontal baffled reactor models: (a) normalized RTD plot and (b) cumulative normalized RTD plot.*

Table 2 shows the US EPA [26] classification of the hydraulic performance of a contact tank based on the baffle factor t_{10}/τ. Thanks to this classification, it is possible to subdivide the performance of

363 the contact tanks in 5 different condition: mixed flow ($t_{10}/\tau < 0.1$), poor condition ($0.1 < t_{10}/\tau < 0.3$),
364 average condition ($0.3 < t_{10}/\tau < 0.5$), superior condition ($0.5 < t_{10}/\tau < 0.7$) and finally plug flow
365 condition when $t_{10}/\tau = 1$

366 **Table 2** *Baffling classification according to the t_{10}/τ index [26].*

Baffling condition	t_{10}/τ
Unbaffled (mixed flow)	0.1
Poor	0.3
Average	0.5
Superior	0.7
Perfect (plug-flow)	1.0

367

368 General regulations instead suggest that Morril (Mo) and dispersion (σ^2) coefficients should be close
369 to 1 and 0 respectively to ensure a perfect mixing and plug-flow condition within the system. From
370 the analysis of the HEI values determined by the CRTD curves in Figure 9b and reported in Table 3,
371 it is possible to observe that for both horizontal baffled geometries, values closer to the ideal have
372 been obtained compared to the conventional geometry. However, as previously observed from the
373 RTD curve, also based on the HEI indices determined by the CRTD curve, the reactor model in which
374 the flow passes through a section that remains constant along the entire path, shows the highest
375 performance.

376 **Table 3** *Hydraulic Efficiency Indicators for conventional and horizontal baffle designs.*

Design	t_{10}/τ	t_{90}/τ	Mo	σ^2
Conventional	0.347	2.000	5.758	1.361
Constant section	0.854	1.253	1.468	0.013
Variable section	0.690	2.270	3.289	0.016

377

378 The improvement of the disinfection in the proposed contact tanks, with horizontal baffles
379 superimposed to the vertical ones, can be attributed to the drastic reduction of the recirculation region.
380 In order to confirm this achieved result, a new geometrical parameter, based on region occupied by
381 the stable reversal flows, is investigated. This parameter is defined as Recirculation Factor (RF) and
382 is calculated according to the following equation:

$$RF = 1 - \frac{V_r}{V_{tot}} \tag{13}$$

383 where V_r is the volume of tank occupied by the recirculation zones and V_{tot} is the overall volume of
384 the reactor.
385 The RF coefficient spans the range [0-1]. It assumes an ideal value of 0 when the entire tank volume
386 is occupied by eddies and dead zones. On the other hand, it is equal to 1 in ideal plug flow conditions,
387 where no recirculation regions occur.
388 In Figure 10, the baffling factor t_{10}/τ has been related to the Recirculation Factor to show how the
389 reduction of the recirculation areas in the tank allows an increase in hydraulic efficiency.
390 Figure 10 shows how the presence of horizontal baffles leads to an increase in the RF compared to
391 traditional multichamber geometries presented in the validation section (NW 4 chambers and HW 8
392 chambers). The insertion of horizontal baffles therefore allows to reduce the volume of recirculation
393 areas improving the reactor hydraulic efficiency. Specifically, in the horizontal baffled reactor with

variable section (Hor_variable) a value of t_{10}/τ equal to 0.690 is achieved for a RF of 0.50, while in the constant section model (Hor_constant), the recirculation reduction allows an increase in RF to a value of 0.63 corresponding to a baffling factor equal to 0.854. Further analysis are required to confirm the validity of the proposed coefficient.

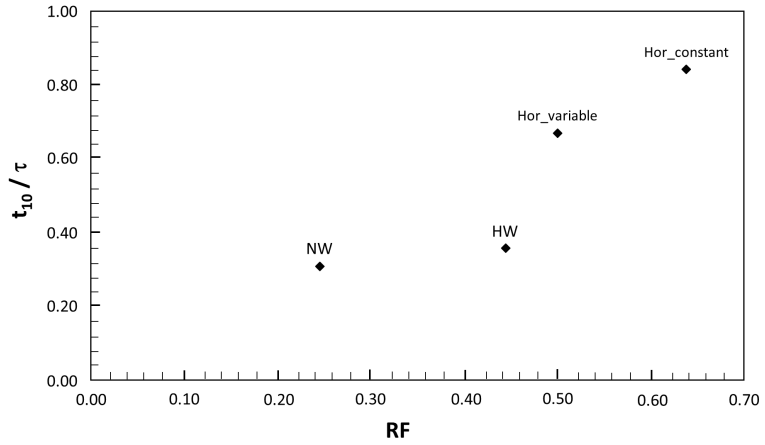


Figure 10 *Relationship between t_{10}/τ and RF coefficients.*

Finally, Figure 11 presents the normalized vertical velocity profiles predicted inside a horizontal chamber for both horizontal baffled designs.

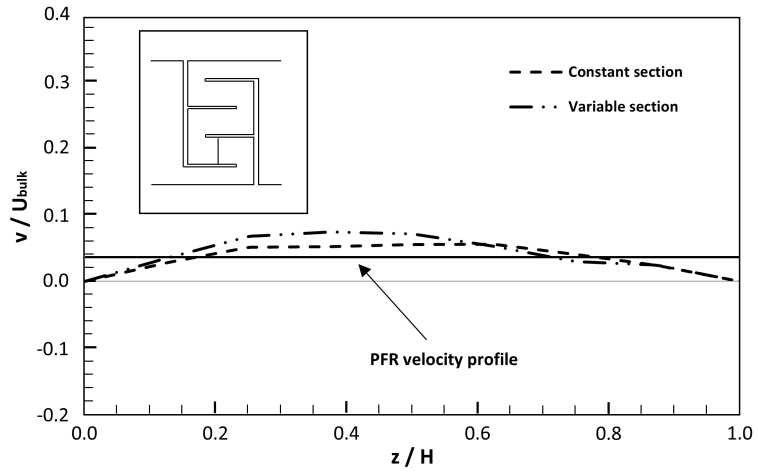


Figure 11 *Vertical velocity component across the chamber height of the two different models.*

As it is possible to observe, for both models the velocity magnitude between two horizontal baffles is close to the ideal plug-flow velocity profile, with a slightly closer trend for the constant section reactor. Furthermore, there are no negative speed values since the geometry does not allow the development of recirculation or dead zones.

5. Conclusions

LES turbulence approach is employed in order to accurately simulate and predict big and small recirculation zones in the tank. Tracer studies show that the conventional tank designs suffer from high short-circuiting and low mixing resulting in poor disinfection efficiency. This study proposes a new contact tank design with horizontal baffles that add to the traditional vertical ones. The new baffles configuration increases the number of flow reversals and reduces the free section for the flow to pass. This results in the reduction of short-circuit phenomena and in the disappearance of the recirculation areas largely present inside the chambers of traditional tanks.

The proposed design is constructively simple to implement as it consists in adding horizontal baffles to the already existing vertical ones. This small constructive device brings the disinfectant residence time in the tank closer to the theoretical HRT, reducing high disinfectant dosage used in traditional chlorine treatment plants, which may be risky for human and public health.

The simulations conducted have shown that by reducing the space between two consecutive horizontal baffles, it is possible to obtain greater hydraulic efficiency. In particular, for the design in which the baffles are arranged in such a way that the flow can pass through a constant section at each point of the tank, a t_{10} index of 0.85 was obtained, much higher than the value of the traditional design ($t_{10} = 0.35$) and very close to the ideal plug-flow value ($t_{10} = 1$).

References

[1] A. Angeloudis, T. Stoesser, C. Gualtieri, R.A. Falconer, Contact Tank Design Impact on Process Performance, Environ. Model. Assess. 21 (2016) 563–576. https://doi.org/10.1007/s10666-016-9502-x.

[2] E. Demirel, M.M. Aral, Unified analysis of multi-chamber contact tanks and mixing efficiency based on vorticity field. part I: Hydrodynamic analysis, Water (Switzerland). 8 (2016) 1–21. https://doi.org/10.3390/w8110495.

[3] A. Angeloudis, T. Stoesser, R.A. Falconer, D. Kim, Flow, transport and disinfection performance in small- and full-scale contact tanks, J. Hydro-Environment Res. 9 (2015) 15–27. https://doi.org/10.1016/j.jher.2014.07.001.

[4] D. Kim, D.-I. Kim, J. Kim, T. Stoesser, Large Eddy Simulation of Flow and Tracer Transport in Multichamber Ozone Contactors, J. Environ. Eng. - J Env. ENG-ASCE. 136 (2010). https://doi.org/10.1061/(ASCE)EE.1943-7870.0000118.

[5] A. Angeloudis, T. Stoesser, R.A. Falconer, Predicting the disinfection efficiency range in chlorine contact tanks through a CFD-based approach, Water Res. 60 (2014) 118–129. https://doi.org/10.1016/j.watres.2014.04.037.

[6] D. Kim, M. Elovitz, P.J.W. Roberts, J.H. Kim, Using 3D LIF to investigate and improve performance of a multichamber ozone contactor, J. / Am. Water Work. Assoc. 102 (2010) 61–70. https://doi.org/10.1002/j.1551-8833.2010.tb10207.x.

[7] Z. Liu, Y.L. Lin, W.H. Chu, B. Xu, T.Y. Zhang, C.Y. Hu, T.C. Cao, N.Y. Gao, C. Di Dong, Comparison of different disinfection processes for controlling disinfection by-product formation in rainwater, J. Hazard. Mater. 385 (2020). https://doi.org/10.1016/j.jhazmat.2019.121618.

[8] J. Jiang, W. Li, X. Zhang, J. Liu, X. Zhu, A new approach to controlling halogenated DBPs by GAC adsorption of aromatic intermediates from chlorine disinfection: Effects of bromide and contact time, Sep. Purif. Technol. 203 (2018). https://doi.org/10.1016/j.seppur.2018.04.050.

[9] J. Zhang, A.E. Tejada-Martinez, H. Lei, Q. Zhang, Indicators for technological, environmental and economic sustainability of ozone contactors, Water Res. 101 (2016). https://doi.org/10.1016/j.watres.2016.06.023.

[10] D. Kim, D.-I. Kim, J.-H. Kim, T. Stoesser, Large Eddy Simulation of Flow and Tracer Transport in Multichamber Ozone Contactors, J. Environ. Eng. 136 (2009) 22–31. https://doi.org/10.1061/(asce)ee.1943-7870.0000118.

[11] J. Zhang, M. Asce, ; A E Tejada-Martínez, Q. Zhang, Hydraulic Efficiency in RANS of the Flow in Multichambered Contactors, (2013). https://doi.org/10.1061/(ASCE)HY.

[12] P. Bruno, G. Di Bella, M. De Marchis, Perforated Baffles for the Optimization of Disinfection Treatment, Water 2020, Vol. 12, Page 3462. 12 (2020) 3462. https://doi.org/10.3390/W12123462.

[13] J. Zhang, A.E. Tejada-Martínez, Q. Zhang, Reynolds-Averaged Navier-Stokes Simulation of the Flow and Tracer Transport in a Multichambered Ozone Contactor, J. Environ. Eng. 139 (2012) 450–454. https://doi.org/10.1061/(asce)ee.1943-7870.0000648.

[14] J. Zhang, A.E. Tejada-Martínez, Q. Zhang, Evaluation of Large Eddy Simulation and RANS for Determining Hydraulic Performance of Disinfection Systems for Water Treatment, J. Fluids Eng. 136 (2014) 121102. https://doi.org/10.1115/1.4027652.
[15] W.B. Rauen, B. Lin, R.A. Falconer, E.C. Teixeira, CFD and experimental model studies for water disinfection tanks with low Reynolds number flows, Chem. Eng. J. 137 (2008) 550–560. https://doi.org/10.1016/J.CEJ.2007.05.011.
[16] E. Demirel, M.M. Aral, An efficient contact tank design for potable water treatment, Tek. Dergi/Technical J. Turkish Chamb. Civ. Eng. 29 (2018) 8279–8294. https://doi.org/10.18400/tekderg.322491.
[17] P. Bruno, G. Di Bella, M. De Marchis, Large Eddy Simulation of Contact Tanks for Disinfection in Drinking Water Treatment, (2020) 503–508. https://doi.org/10.1007/978-3-030-42822-8_66.
[18] M. De Marchis, Large eddy simulations of roughened channel flows: Estimation of the energy losses using the slope of the roughness, Comput. Fluids. 140 (2016) 148–157. https://doi.org/https://doi.org/10.1016/j.compfluid.2016.09.021.
[19] P. Ouro, B. Fraga, N. Viti, A. Angeloudis, T. Stoesser, C. Gualtieri, Instantaneous transport of a passive scalar in a turbulent separated flow, Environ. Fluid Mech. 18 (2018) 487–513. https://doi.org/10.1007/s10652-017-9567-3.
[20] J. Zhang, A.E. Tejada-Martínez, Q. Zhang, Developments in computational fluid dynamics-based modeling for disinfection technologies over the last two decades: A review, Environ. Model. Softw. 58 (2014) 71–85. https://doi.org/10.1016/j.envsoft.2014.04.003.
[21] D. Kim, T. Stoesser, J.H. Kim, Modeling aspects of flow and solute transport simulations in water disinfection tanks, Appl. Math. Model. 37 (2013) 8039–8050. https://doi.org/10.1016/j.apm.2013.03.031.
[22] J. Zhang, A.E. Tejada-Martínez, Q. Zhang, Reynolds-averaged Navier-Stokes Simulation of the flow and tracer transport in a multichambered ozone contactor, J. Environ. Eng. (United States). 139 (2013) 450–454. https://doi.org/10.1061/(ASCE)EE.1943-7870.0000648.
[23] M.M. Aral, E. Demirel, Novel Slot-Baffle Design to Improve Mixing Efficiency and Reduce Cost of Disinfection in Drinking Water Treatment, J. Environ. Eng. 143 (2017) 06017006. https://doi.org/10.1061/(asce)ee.1943-7870.0001266.
[24] E.C. Teixeira, R. Do Nascimento Siqueira, Performance assessment of hydraulic efficiency indexes, J. Environ. Eng. 134 (2008) 851–859. https://doi.org/10.1061/(ASCE)0733-9372(2008)134:10(851).
[25] D.M. Marske, J.D. Boyle, Chlorine Contact Chamber Design - A Field Evaluation. Water and Sewage Works 120 (1973) 70-77.
[26] United States Environmental Protection Agency. Disinfection Profiling and Benchmarking Guidance Manual; Appendix A Rep. No. EPA 816-R-03-004 EPA; USEPA: Cincinnati, OH, USA, 1999.